

## Far-forward collective scattering measurements of density fluctuations in the helically symmetric experiment stellarator)

C. B. Deng and D. L. Brower

Citation: [Review of Scientific Instruments](#) **81**, 10D503 (2010); doi: 10.1063/1.3464471

View online: <http://dx.doi.org/10.1063/1.3464471>

View Table of Contents: <http://scitation.aip.org/content/aip/journal/rsi/81/10?ver=pdfcov>

Published by the [AIP Publishing](#)

---

### Articles you may be interested in

[Core density gradient fluctuation measurement by differential interferometry in the helically symmetric experiment stellarator\)](#)

Rev. Sci. Instrum. **83**, 10E308 (2012); 10.1063/1.4730999

[Density fluctuation measurements by far-forward collective scattering in the MST reversed-field pincha\)](#)

Rev. Sci. Instrum. **83**, 10E302 (2012); 10.1063/1.4728098

[Poloidal beam emission spectroscopy system for the measurement of density fluctuations in Large Helical Devicea\)](#)

Rev. Sci. Instrum. **81**, 10D719 (2010); 10.1063/1.3478685

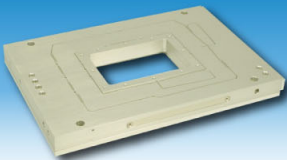
[Beam emission spectroscopy measurement for density fluctuations in compact helical system](#)

Rev. Sci. Instrum. **75**, 4118 (2004); 10.1063/1.1794846

[Lithium beam probe for edge density profile measurements on the large helical device](#)

Rev. Sci. Instrum. **74**, 1865 (2003); 10.1063/1.1538343

---



Nanopositioning Systems      Micropositioning      AFM & SPM      Single molecule imaging

# Far-forward collective scattering measurements of density fluctuations in the helically symmetric experiment stellarator<sup>a)</sup>

C. B. Deng and D. L. Brower<sup>b)</sup>

*Department of Physics, University of California, Los Angeles, California 90095, USA*

(Presented 17 May 2010; received 12 May 2010; accepted 9 June 2010; published online 1 October 2010)

The multichannel interferometer system on the helically symmetric experiment (HSX) stellarator is reconfigured to perform far-forward collective scattering measurements of electron density fluctuations. The collective scattering system has nine viewing chords with 1.5 cm spacing. Scattered power is measured using a homodyne detection scheme. Far-forward collective scattering provides a line-integrated measurement of fluctuations within the divergence of the probe beam covering wavenumber range:  $k_{\perp} < 2 \text{ cm}^{-1}$ . The perpendicular wavenumber consists of poloidal and radial contributions that vary with chord position. Both coherent modes and broadband fluctuation are measured. When HSX is operated without quasihelical symmetry at  $B_T=1 \text{ T}$  and  $n_e \sim 4 \times 10^{12} \text{ cm}^{-3}$ , a coherent electrostatic fluctuation is observed. © 2010 American Institute of Physics. [doi:10.1063/1.3464471]

## I. INTRODUCTION

The helically symmetric experiment (HSX) is a stellarator optimized to reduce neoclassical transport in the low collisionality regime by having a magnetic field strength that is constant in a helical direction on a flux surface.<sup>1</sup> As a consequence, confinement in the quasihelically symmetric stellarator can be dominated by anomalous transport associated with plasma instabilities and turbulence. This motivates the need for direct measurements of fluctuations in the core of the HSX device. Experimental results can be used to compare with neoclassical and turbulent transport modeling. To that end, the multichannel interferometer system routinely used to measure the line-integrated density profile has been modified in order to include a far-forward collective scattering capability for the measurement of electron density fluctuations. Far-forward scattering measures collective scattering within the divergence of the probing electromagnetic wave.<sup>2</sup> On HSX, this technique has been successfully used to measure both coherent modes associated with energetic particle driven instabilities as well as broadband density fluctuations. The system will be described along with initial results. Comparison of fluctuations measured using both far-forward collective scattering and interferometry will be made. Future plans for large angle scattering will also be detailed.

## II. FAR-FORWARD COLLECTIVE SCATTERING

The optical layout for the multichannel interferometer system on HSX is shown in Fig. 1. The source is a bias-tuned Gunn diode at 96 GHz with passive solid-state tripler providing output at 288 GHz ( $\sim 5 \text{ mW}$ ). It can be frequency-

modulated so that heterodyne detection at the modulation frequency of  $\sim 1 \text{ MHz}$  is possible.<sup>3</sup> In this configuration, the output beam is roughly equally divided into two parts serving as the probe and local oscillator (LO) beams, respectively. Each beam is expanded using parabolic beam expansion optics such that the size is essentially the available port view of  $2.5 \times 13.5 \text{ cm}^2$ . This probe beam, after passing through the plasma, illuminates a linear detector array, containing nine Schottky-diode corner-cube mixers. The linear array also receives rf bias from the LO beam. High-density polyethylene lens of width  $w=1.5 \text{ cm}$  are used to focus the radiation onto each sensing element. In this arrangement, the expanded beam is effectively subdivided into nine discrete chords which span most of the plasma cross section. Phase changes in the 1 MHz beat signal with respect to a reference provide information on the line-integrated density profile. This system has been implemented to measure the electron density distribution in HSX.<sup>3,4</sup>

While interferometer systems have been successfully employed to measure density fluctuations (typically coherent modes) as well as the equilibrium density profile, in an effort to improve sensitivity we have recently operated the diagnostic in a mode whereby far-forward collective scattering from the electromagnetic probe wave is measured. As opposed to the interferometer approach which measures phase, for scattering one measures the amplitude of the scattered wave. To accomplish this measurement, one only needs to remove the frequency modulation of the source which converts the probe and LO beams to continuous equivalent frequencies for homodyne detection. For initial tests, the amplifier system used for the detected scattered radiation (same as used for interferometry) was not optimized for flat response at frequencies  $< 100 \text{ kHz}$  requiring application of an instrument function correcting for amplifier filtering. It should be noted that in this configuration simultaneous interferometer measurements are not possible. Far-forward collective scat-

<sup>a)</sup> Contributed paper, published as part of the Proceedings of the 18th Topical Conference on High-Temperature Plasma Diagnostics, Wildwood, New Jersey, May 2010.

<sup>b)</sup> Electronic mail: brower@ucla.edu.

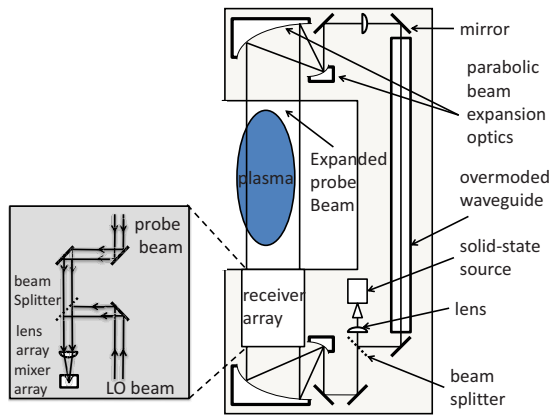


FIG. 1. (Color online) Optical layout for HSX interferometer and far-forward scattering system.

tering provides a line-integrated measurement of fluctuations within the divergence of the probe beam covering wavenumber range:  $k_{\perp} < 2 \text{ cm}^{-1} (= \pi/w)$ . The perpendicular wavenumber  $k_{\perp}$  (perpendicular to the magnetic field) consists of both poloidal and radial contributions which vary with chord position.

An example of the measured scattered signals for four chords at different impact parameters ( $R-R_0$ ) is shown in Fig. 2, for a HSX discharge with  $B_T=1 \text{ T}$ ,  $n_e \sim 4-7 \times 10^{12} \text{ cm}^{-3}$  and 100 kW of electron cyclotron resonance heating (ECRH) power. For each chord, scattered radiation, proportional to the square of the density fluctuation amplitude [ $P_{\text{scat}} \propto \tilde{n}^2$ ], is measured throughout the duration of the plasma which is determined by the length of the ECRH heating pulse, 50 ms. Fluctuation temporal evolution for edge and central chords are different indicating a change in the spatial distribution with time. The corresponding frequency power spectra for a 5 ms time window during (solid) and before (dashed) the plasma discharge are shown in Fig. 3(a). Data are sampled at 1 MHz. Across the entire spectrum from 20 to 200 kHz, broadband density fluctuations are measured. The most distinguishing feature is a large coherent mode at  $\sim 30 \text{ kHz}$  which is observed to peak for chords located 2–4 cm away from plasma center, where the density gradient is steepest. For comparison, the frequency power spectra for the interferometric measurement are also shown for the same chord and similar plasma conditions. Interferometer bandwidth is limited to 200 kHz due to noise associated with

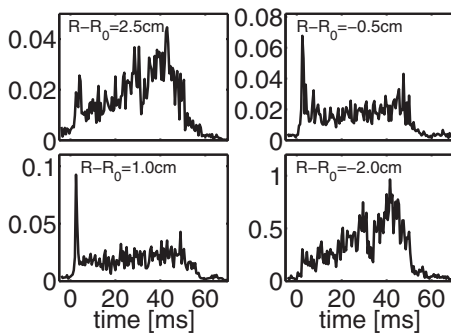


FIG. 2. Scattered power (arbitrary units) for chords with various impact parameters,  $R-R_0$ .

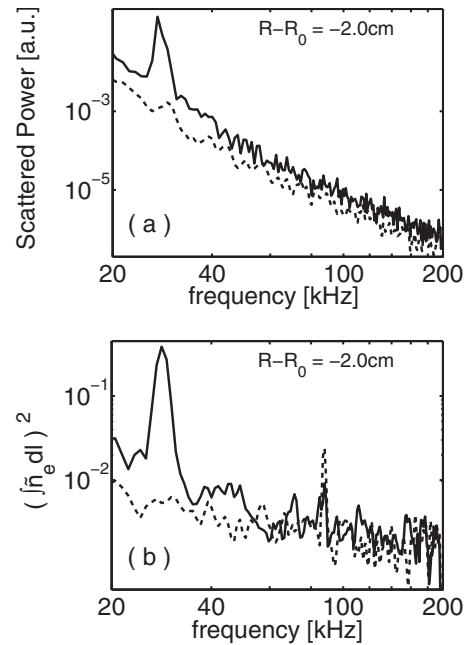


FIG. 3. Density fluctuation frequency spectra for similar plasmas comparing measurements by (a) far-forward collective scattering and (b) interferometry. Solid line is with plasma and dashed line is without.

frequency-modulating the source. Both techniques clearly resolve the low-frequency coherent mode but far-forward scattering is better suited to measure the higher-frequency broadband fluctuations,  $>50 \text{ kHz}$ .

Strong signal levels enable the diagnostic to track changes in the density fluctuations throughout the plasma duration. In Fig. 4, time evolution of the power spectra indicates that multiple coherent modes appear with the application of dc bias to an inserted probe which modifies the plasma potential. During the time of biasing, 30–40 ms, modes appear on the density fluctuation spectra at approximately 20, 40, 130, and 180 kHz. Some, but not all, of these same fluctuations are also measured by an edge magnetic coil. These coherent modes may be related to energetic electron driven instabilities linked to acoustic modes previously identified in quasihelically symmetric (QHS) plasmas at  $B_T = 0.5 \text{ T}$ .<sup>5</sup> Future work will focus on studying these modes as well as broadband turbulence and their dependence on magnetic configuration and biasing. As shown in Fig. 5, a broad spectrum (up to 500 kHz) of density fluctuations can be iden-

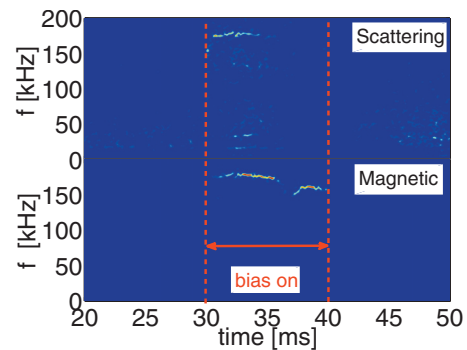


FIG. 4. (Color) Far-forward scattering power spectra at  $R-R_0=1.0 \text{ cm}$  during discharge with dc bias applied to modify plasma potential.

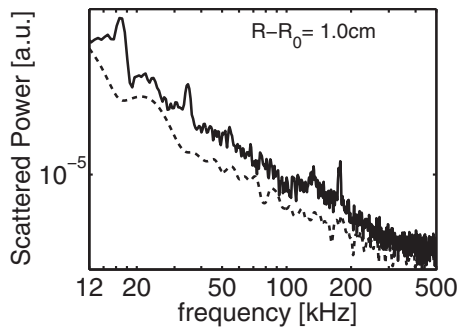


FIG. 5. Density and fluctuation frequency spectra for QHS plasma with  $B = 1$  T: system noise (dashed line) and broadband density fluctuations (solid line). Same shot as that shown in Fig. 4.

tified. Multiple coherent modes appear with positive biasing (30–40 ms). Information on their spatial distribution can be obtained by comparing spectra from chords with different impact parameters. Studies of these fluctuations can impact investigations of both anomalous transport and plasma/zonal flows.

### III. FUTURE PLANS

Future plans call for reconfiguring the existing system to accommodate interferometry and scattering simultaneously. A schematic of this setup is shown in Fig. 6. The beams from two  $\sim 300$  GHz sources ( $f_1 - f_2 \sim 1$  MHz) serve as the probe and LO beams. In this configuration, there are two detected signals corresponding to far-forward scattering and conventional collective scattering where the conventional scattered radiation is at angle  $\theta_s$ , much larger than the divergence of the probe beam. In this orientation the fluctuation  $k_{\perp}$  can be related to the incident beam and  $\theta_s$  via the Bragg relation:  $k_{\perp} = 2k_o \sin(\theta_s/2)$ , where  $k_o = 2\pi/\lambda_o \sim 60$   $\text{cm}^{-1}$ .

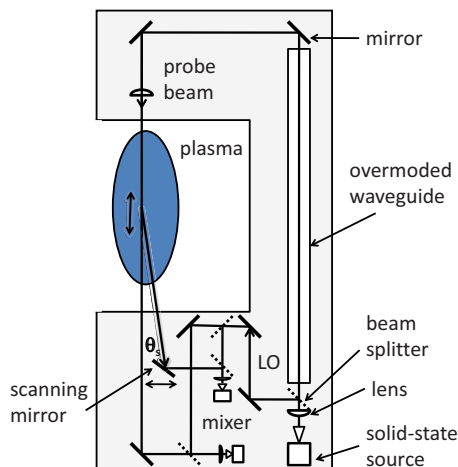


FIG. 6. (Color online) Schematic of combined single channel interferometer and collective scattering system.

Whereas far-forward scattering is limited to wave vectors  $< 2$   $\text{cm}^{-1}$ , the configuration in Fig. 6 allows for measurement of fluctuations at higher  $k_{\perp}$ . For instance, for  $\theta_s = 5^\circ$ ,  $k_{\perp} \sim 5.3$   $\text{cm}^{-1}$ . Scattering angle can be varied by rotating the scanning mirror to investigate a wide range of  $k_{\perp}$ , including both large and small spatial-scale fluctuations. Adding a second scattering channel with different  $\theta_s$  is also possible. With larger  $\theta_s$ , the measurement becomes more spatially resolved ( $L_v = 2w/\sin \theta_s$ ), e.g.,  $\theta_s = 10^\circ$  corresponds to  $L_v \sim 17$  cm and  $k_{\perp} = 10$   $\text{cm}^{-1}$ . With this resolution, one could resolve the plasma core and edge regions. Horizontally scanning the collection mirror (say between shots) allows one to move the sample volume along the vertical chord and map out the spatial distribution of the fluctuation. In addition, the measured fluctuation frequency, in the laboratory frame of reference, consists of both the mode frequency and a Doppler shift due to  $E \times B$  flows,  $\omega_{\text{measured}} = \omega_{\text{mode}} + k_{\perp} E_r / B$ . This allows one to relate shifts in the spectra to changes in  $E_r$  provided the mode frequency is small. One could use this characteristic of the scattered signal to determine whether the HSX equilibrium has electron or ion root confinement as the large  $E_r$  variation between these two roots would lead to large changes in the frequency spectra.

The heterodyne detection scheme allows measurements of wave propagation direction as well as unambiguous determination of plasma density, simultaneously. For interferometry, an additional reference mixer (not shown) is required to monitor the  $\sim 1$  MHz beat wave (without plasma) and make the phase measurement. Heterodyne detection also has lower noise, thereby enabling measurement of smaller amplitude density perturbations. The combined interferometry-scattering system would provide a single chord of density (and far-forward scattering) information while large-angle scattering could be achieved at multiple angles.

### ACKNOWLEDGMENTS

This work is supported by the Department of Energy under Grant Nos. DE-FG02-01ER-54615 Task II and DE-FG02-93ER54222.

- <sup>1</sup>F. S. B. Anderson, D. T. Anderson, A. F. Almagri, J. Chen, S. Gerhardt, V. Sakaguchi, J. Shafii, and J. N. Talmadge, Proceedings of the 12th International Stellarator Conference, Madison, Wisconsin, 27 September–1 October 1999.
- <sup>2</sup>D. E. Evans, E. J. Doyle, D. Frigione, M. von Hellermann, and A. Murdoch, *Plasma Phys.* **25**, 617 (1983).
- <sup>3</sup>D. L. Brower, C. Deng, and W. X. Ding, *Rev. Sci. Instrum.* **72**, 1081 (2001).
- <sup>4</sup>C. Deng, D. L. Brower, W. X. Ding, A. F. Almagri, D. T. Anderson, F. S. B. Anderson, S. P. Gerhardt, P. Probert, and J. N. Talmadge, *Rev. Sci. Instrum.* **74**, 1625 (2003).
- <sup>5</sup>C. Deng, D. L. Brower, B. N. Breizman, D. A. Spong, A. F. Almagri, D. T. Anderson, F. S. B. Anderson, W. X. Ding, W. Guttenfelder, K. M. Likin, and J. N. Talmadge, *Phys. Rev. Lett.* **103**, 025003 (2009).